

# Glass transition and crystallization kinetics analysis of Sb–Se–Ge chalcogenide glasses

Sunanda Sharda · Neha Sharma · Pankaj Sharma · Vineet Sharma

Received: 27 November 2012 / Accepted: 9 April 2013 / Published online: 17 May 2013  
© Akadémiai Kiadó, Budapest, Hungary 2013

**Abstract** Differential thermal analysis (DTA) has been employed to investigate the effect of Ge addition on the glass transition behavior and crystallization kinetics of  $\text{Sb}_{10}\text{Se}_{90-x}\text{Ge}_x$  ( $x = 0, 19, 21, 23, 25, 27$ ) alloys. The three characteristic temperatures viz. glass transition ( $T_g$ ), crystallization ( $T_c$ ), and melting ( $T_m$ ) have been determined and found to vary with the heating rates and Ge content. Thermal stability and glass forming tendency have been evaluated in terms of  $\Delta T (= T_c - T_g)$  and reduced glass transition temperature. The activation energies for glass transition and crystallization have been used to analyze the nucleation and growth process. The activation energy analysis also determines the suitability of alloys to be used in switching applications. Results have been interpreted in terms of bond energies and structural transformations in the investigated alloys.

**Keywords** Non-isothermal kinetics · Glass transition kinetics · Activation energy · Cohesive energy

## Introduction

The thermal stability of chalcogenide glasses is related to the nucleation and growth processes which in turn depend

on glass transition and crystallization kinetics [1]. The two processes glass transition and crystallization, limit the applications of inorganic glassy materials. Chalcogenide glasses can be potentially used in threshold and memory switching devices [2, 3]. Glassy alloys must be stable in the amorphous state at low temperature and should have a short crystallization time to be used as an optical recording media [4]. The switching properties depend upon crystallization temperature ( $T_c$ ) and hence, the thermal stability of the glasses. These characteristics rely on the composition of the system. Higher the value of  $T_c$  for a particular composition more will be the thermal stability of the glass [5] and therefore, better will be its suitability for applications.

Amorphous Se deteriorates in xerographic properties near glass transformation region [6]. Adding Sb to Se leads to greater hardness, higher sensitivity, conductivity and smaller ageing effects in comparison to pure a–Se [7]. The a–SbSe glass has potential applications in photoconductive elements [8]. But, these properties are restricted by the rapid crystallization of stoichiometric composition  $\text{Sb}_2\text{Se}_3$  [9]. Sb–Se glasses can be stabilized by adding Ge, as the physical and optical properties change, when it substitutes Se atoms and hence may increase the stability [10, 11]. In  $\text{Sb}_{10}\text{Se}_{90-x}\text{Ge}_x$  system,  $x = 25$  shows highest optical band gap, and structure stability [10–12]. So, the thermal study of  $\text{Sb}_{10}\text{Se}_{90-x}\text{Ge}_x$  system may present an insight into the configurational and conformational changes.

The paper deals with the study of glass-crystal transformation of  $\text{Sb}_{10}\text{Se}_{90-x}\text{Ge}_x$  ( $x = 0, 19, 21, 23, 25, 27$ ) alloys. Differential thermal analysis has been used to determine the glass transition ( $T_g$ ), crystallization ( $T_c$ ), and melting ( $T_m$ ) temperature of alloys. Non-isothermal technique is used instead of isothermal technique as it can be performed rapidly and the temperature range of measurements can be

---

S. Sharda · N. Sharma · P. Sharma (✉) · V. Sharma  
Department of Physics and Materials Science, Jaypee University  
of Information Technology, Waknaghat,  
Solani 173234, HP, India  
e-mail: pks\_phy@yahoo.co.in

S. Sharda  
e-mail: sunandasharda@gmail.com

V. Sharma  
e-mail: vneetsharma@gmail.com

extended. The thermal stability and glass forming tendency have been studied in terms of  $\Delta T (= T_c - T_g)$  and reduced glass transition temperature ( $T_{rg}$ ). Heating rate dependence of  $T_g$  has been evaluated. The activation energy of glass transition has been determined by Moynihan's method and Kissinger's method. The activation energy of crystallization has been calculated using Mahadevan's method and Augis-Bennett method. The results using different methods have been analyzed and compared.

## Experimental

Bulk samples of  $Sb_{10}Se_{90-x}Ge_x$  ( $x = 0, 19, 21, 23, 25, 27$ ) were prepared using melt quench technique. The detailed experimental procedure for sample preparation is given elsewhere [11]. The composition of the bulk samples was analyzed using a scanning electron microscope (SEM) (Zeiss EVO 40 EP with EDAX attachment operated at 20 kV). The amorphous state of the alloys was confirmed by the absence of sharp peaks in the X-ray diffraction peaks (X'Pert PRO) [11]. The thermal behavior of the samples was investigated using DTA (EXSTAR TG/DTA 6300). DTA runs were taken at four different heating rates 5, 10, 15, and 20  $K\ min^{-1}$ . For each run, approximately 10 mg of the sample was taken in alumina pans in an atmosphere of dry nitrogen at a flow rate of 200  $mL\ min^{-1}$  under non-isothermal conditions. The analyzer was calibrated prior to the measurements using the known latent heats of high purity elements zinc, indium and lead. The temperature precision of microprocessor of thermal analyzer was  $\pm 0.1\ K$ .

## Results and discussion

EDAX indicates that the atomic mass percentages of the constituent elements are close to their starting elements (Table 1).

In the studied temperature range for DTA, three characteristic peaks are observed. The first endothermic peak corresponds to  $T_g$ , second exothermic peak to  $T_c$  and third

endothermic peak to melting  $T_m$ .  $T_g$  represents the rigidity of the system. Hence, it provides valuable information about the thermal stability of the glass. Crystallization process is a heating rate dependent phenomenon because nucleation is a thermally activated process whereas  $T_g$  depends on heating rate ( $\alpha$ ) due to relaxation processes [1]. Figures 1, 2 and 3 shows the three characteristic temperatures for  $Sb_{10}Se_{90-x}Ge_x$  ( $x = 0, 19, 21, 23, 25, 27$ ) samples at different heating rates. The difference between  $T_g$  and  $T_c$  increases with an increase in  $Ge$  alloying concentration, pointing toward the stability of the system. The three parameters,  $T_g$ ,  $T_c$ , and  $T_m$  increase with increase in heating rate for all the samples.  $T_g$  attains maximum value for  $Sb_{10}Se_{65}Ge_{25}$  because  $Ge$  on entering the polymeric structure of  $Sb_{10}Se_{90}$  forms tetrahedral  $Ge(Se_{1/2})_4$  units, in addition to trigonal  $Sb_2Se_3$  units, replacing the  $Se-Se$  bonds [12]. At  $x = 25$ , the system becomes heavily cross linked with the formation of  $Sb_2Se_3$  and  $Ge(Se_{1/2})_4$  units only and becomes completely rigid. On further increase of  $Ge$  content, at  $x = 27$ , the system contains homopolar  $Ge-Ge$  bonds in addition to  $Sb_2Se_3$  and  $Ge(Se_{1/2})_4$  structural units, thereby decreasing  $T_g$  [12].

The thermal stability factor,  $\Delta T$  [13], indicates thermal stability of the glass. The ease of glass formation can also be determined by evaluating  $T_{rg} (= T_g/T_m)$  values which obey two-third rule [14]. The  $T_{rg}$  values are found to be of the order of 2/3 (Table 2) indicating a good glass forming

**Table 1** Elemental composition of bulk glasses

| Composition             | Sb    | Se    | Ge    |
|-------------------------|-------|-------|-------|
| $Sb_{10}Se_{90}$        | 10.83 | 89.17 | 0     |
| $Sb_{10}Se_{71}Ge_{19}$ | 9.86  | 71.56 | 18.58 |
| $Sb_{10}Se_{69}Ge_{21}$ | 9.96  | 69.84 | 20.20 |
| $Sb_{10}Se_{67}Ge_{23}$ | 10.10 | 67.73 | 22.17 |
| $Sb_{10}Se_{65}Ge_{25}$ | 10.37 | 64.13 | 25.50 |
| $Sb_{10}Se_{63}Ge_{27}$ | 10.41 | 61.85 | 27.74 |

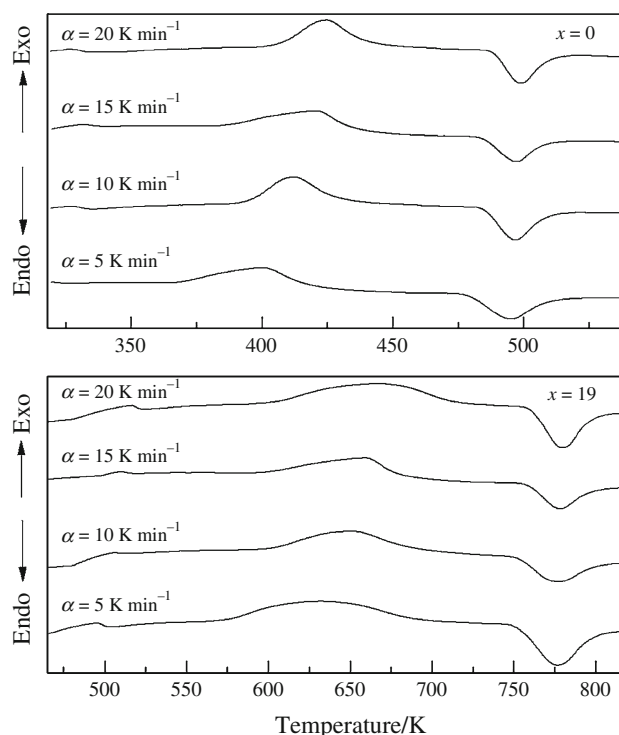


**Fig. 1** DTA traces of  $Sb_{10}Se_{90}$  and  $Sb_{10}Se_{71}Ge_{19}$  glassy alloys at heating rates 5, 10, 15 and 20  $K\ min^{-1}$

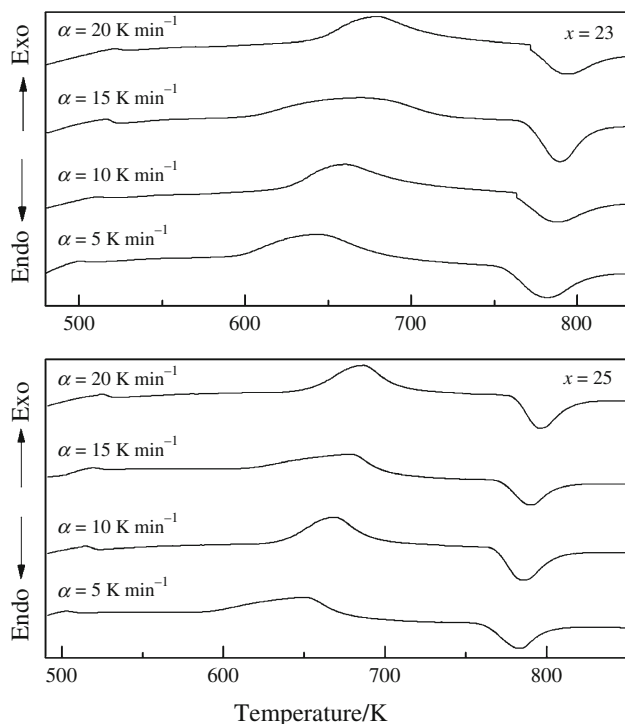


**Fig. 2** DTA thermograms for  $\text{Sb}_{10}\text{Se}_{69}\text{Ge}_{21}$  and  $\text{Sb}_{10}\text{Se}_{67}\text{Ge}_{23}$  glassy alloys at heating rates 5, 10, 15 and 20  $\text{K min}^{-1}$

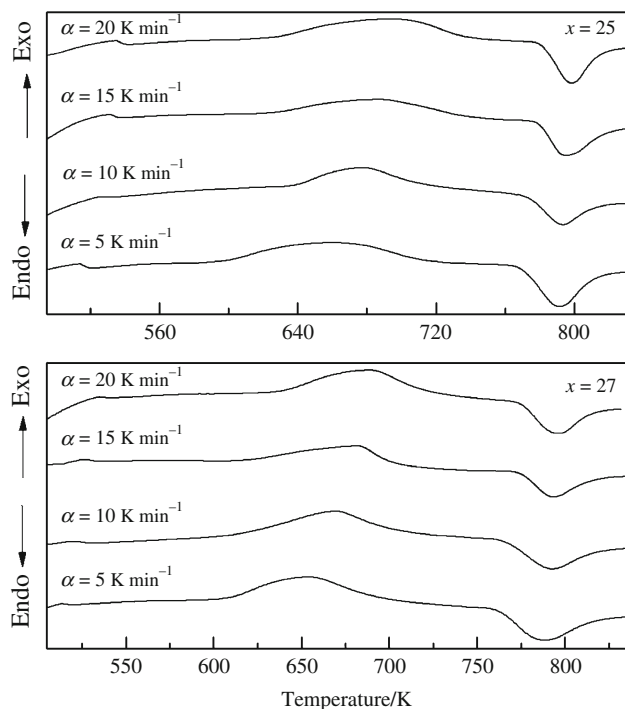


**Fig. 3** DTA scans of  $\text{Sb}_{10}\text{Se}_{65}\text{Ge}_{25}$  and  $\text{Sb}_{10}\text{Se}_{63}\text{Ge}_{27}$  glassy alloy at heating rates 5, 10, 15 and 20  $\text{K min}^{-1}$

tendency of the material. The values of  $\Delta T$  increase with increase in Ge content showing maximum at 25 at.% Ge and then decreases for 27 at.% (Table 2). The kinetic

**Table 2** Values of glass transition ( $T_g$ ), crystallization ( $T_c$ ), melting ( $T_m$ ) temperatures, thermal stability parameter ( $\Delta T$ ) and reduced glass transition temperature ( $T_{rg}$ ) at 10  $\text{K/min}$  for  $\text{Sb}_{10}\text{Se}_{90-x}\text{Ge}_x$  ( $x = 0, 19, 21, 23, 25, 27$ ) glassy alloys

| Sample   | $T_g/\text{K}$ | $T_c/\text{K}$ | $T_m/\text{K}$ | $\Delta T/\text{K}$ | $T_{rg}$ |
|----------|----------------|----------------|----------------|---------------------|----------|
| $x = 0$  | 335.45         | 412.48         | 496.59         | 77.03               | 0.6755   |
| $x = 19$ | 512.71         | 650.91         | 777.04         | 138.20              | 0.6598   |
| $x = 21$ | 518.45         | 660.61         | 788.37         | 142.16              | 0.6576   |
| $x = 23$ | 523.36         | 669.37         | 786.17         | 146.01              | 0.6657   |
| $x = 25$ | 531.47         | 678.74         | 793.71         | 147.27              | 0.6696   |
| $x = 27$ | 530.28         | 670.30         | 792.71         | 140.02              | 0.6689   |

resistance to crystallization increases with increase in the  $\Delta T$  values. This leads to a slowdown of nucleation rate due to the increase in viscosity of the system [15]. Thus,  $\text{Sb}_{10}\text{Se}_{65}\text{Ge}_{25}$  shows maximum thermal stability and lower crystallizing ability.

The heating rate dependence of  $T_g$  can be evaluated using the empirical relation [16],

$$T_g = A + B \ln \alpha, \quad (1)$$

where  $A$  indicates  $T_g$  at a heating rate of 1  $\text{K min}^{-1}$  and  $B$  is related to the cooling rate of the melt. The values of  $A$  and  $B$  (Table 3) have been determined from the intercept and slope respectively, in Fig. 4.  $A$  shows variation similar to that of  $T_g$ , obtained from the DTA thermograms.  $B$  corresponds to the time response of configurational changes within the glass transition region to the heating rate. The values of activation energy of glass transition ( $E_g$ ) have been calculated from heating rate dependence of  $T_g$  using two methods [17, 18].

In the first method, the heating rate dependence of  $T_g$  in terms of thermal relaxation phenomenon is given by Moynihan et al. [17] as,

$$d(\ln \alpha)/d\left(\frac{1}{T_g}\right) = -E_g/R, \quad (2)$$

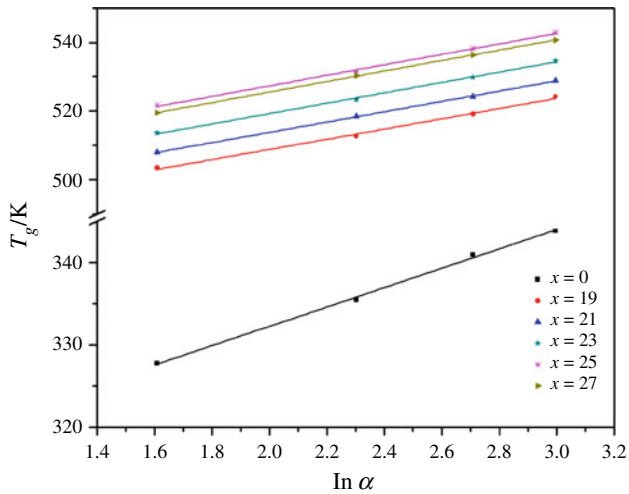
where  $E_g$  is activation energy of glass transition and  $R$  is gas constant. The slope of  $\ln \alpha$  versus  $1,000/T_g$  graph in Fig. 5a gives the activation energy involved in molecular motions and rearrangements around  $T_g$ . The slope increases with rise in the Ge content to maximum at 25 at.% Ge alloying and decreases with further Ge addition. Activation energy values obtained depend on the thermal history of the sample as the thermal relaxation depends on the temperature as well as structure.

The dependence of  $T_g$  on heating rate can also be found using Kissinger's equation [18], suggested for crystallization processes with spherical nuclei and having less dependence on thermal history of the sample, as,

$$\ln\left(\frac{\alpha}{T_g^2}\right) = -E_g/RT_g + \text{constant}, \quad (3)$$

**Table 3** Values of  $A$ ,  $B$ , activation energies for  $\text{Sb}_{10}\text{Se}_{90-x}\text{Ge}_x$  ( $x = 0, 19, 21, 23, 25, 27$ ) glassy alloys

| Sample   | $A/K$  | $B$   | $E_g/\text{kJ mol}^{-1}$ [17] | $E_g/\text{kJ mol}^{-1}$ [18] | $E_c/\text{kJ mol}^{-1}$ [20] | $E_c/\text{kJ mol}^{-1}$ [21] |
|----------|--------|-------|-------------------------------|-------------------------------|-------------------------------|-------------------------------|
| $x = 0$  | 308.76 | 11.74 | 79.62                         | 73.97                         | 79.21                         | 75.80                         |
| $x = 19$ | 479.01 | 14.89 | 146.76                        | 138.20                        | 137.78                        | 132.37                        |
| $x = 21$ | 483.84 | 14.98 | 148.84                        | 140.19                        | 142.11                        | 136.61                        |
| $x = 23$ | 489.15 | 15.06 | 151.26                        | 142.60                        | 144.77                        | 139.19                        |
| $x = 25$ | 496.68 | 15.32 | 153.34                        | 144.52                        | 147.85                        | 142.19                        |
| $x = 27$ | 494.93 | 15.29 | 152.51                        | 143.69                        | 146.52                        | 140.94                        |

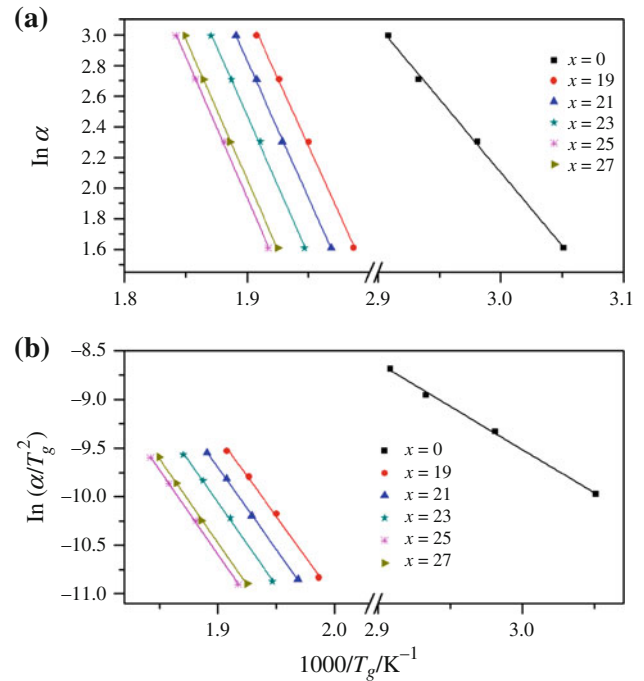
**Fig. 4** Dependence of glass transition temperature ( $T_g$ ) on heating rate ( $\alpha$ ) for  $\text{Sb}_{10}\text{Se}_{90-x}\text{Ge}_x$  ( $x = 0, 19, 21, 23, 25, 27$ ) glassy alloys

where  $R$  is gas constant. The activation energy values obtained from Fig. 5b are in good agreement with those obtained using Moynihan's method, with a maximum in  $E_g$  at  $x = 25$ .

Variation in values of activation energy calculated (Table 3) by different methods is due to dissimilar approximations used in the models. On heating the sample in DTA furnace, atoms undergo transitions between the local potential minima having different characteristic structures in the configuration space and energy barriers. The internal energy associated with the most stable local minimum is lowest and hence, corresponds to the most stable structure. The atoms can jump more easily to these metastable states [19].

The crystallization involves three types of activation energies *i.e.*, nucleation, growth and whole crystallization process. The activation energy for growth may be taken equal to the crystallization process, provided it is evaluated using thermal analysis. Activation energy of crystallization ( $E_c$ ) has been evaluated using different approaches given by [20, 21].

Firstly, Mahadevan et al. [20] have proposed an approximation for the calculation of  $E_c$  using,

**Fig. 5** Plot of **a**  $\ln \alpha$  versus  $1000/T_g$ , **b**  $\ln(\alpha/T_g^2)$  versus  $1000/T_g$  for  $\text{Sb}_{10}\text{Se}_{90-x}\text{Ge}_x$  ( $x = 0, 19, 21, 23, 25, 27$ ) glassy alloys

$$\ln \alpha = -E_c/RT_c + \text{constant} \quad (4)$$

The activation energy is evaluated from the slopes in Fig. 6a and found to be maximum for  $x = 25$  at.%.

In second approach, Augis and Benett [21] also suggested a method for the evaluation of crystallization activation energy using relation,

$$\ln(\alpha/T_c) = -E_c/RT_c + \ln K_0, \quad (5)$$

where  $K_0$  is the frequency factor. This method is preferred over other methods as the values of kinetic parameter  $K_0$  in addition to  $E_c$  can be obtained. The slope in this relation gives the value of  $E_c$ . The value of  $E_c$  increases to maximum as Ge is added to  $\text{Sb}_{10}\text{Se}_{90}$  till 25 at.% alloying and then decreases as shown in Fig. 6b.

The values of  $E_c$  calculated using different methods are found to be in good agreement with each other (Table 3).

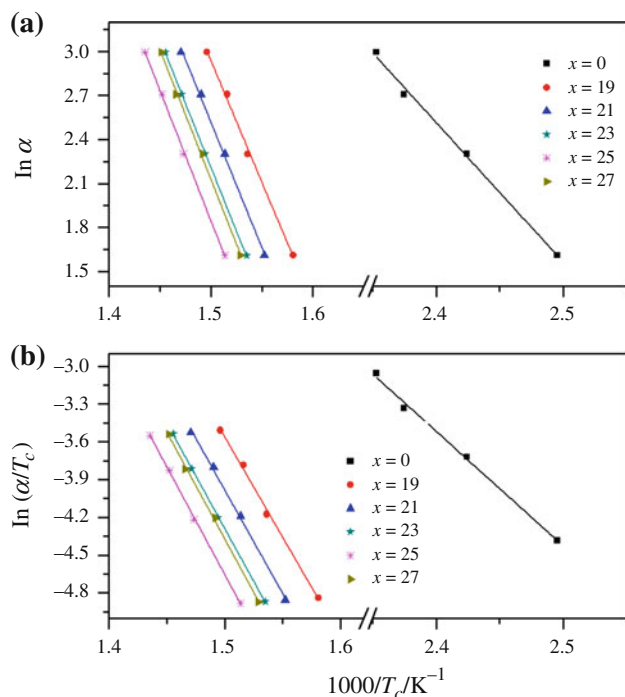


**Fig. 6** Variation of **a**  $\ln \alpha$  with  $1,000/T_c$ , **b**  $\ln (\alpha/T_c)$  with  $1,000/T_c$  for  $\text{Sb}_{10}\text{Se}_{90-x}\text{Ge}_x$  ( $x = 0, 19, 21, 23, 25, 27$ ) glassy alloys

The variation in  $E_c$  values may be interpreted in terms of bond energies of the system. The bond energy of the heteropolar bond is [22],

$$E_{A-B} = (E_{A-A} \times E_{B-B})^{0.5} + 30(\chi_A - \chi_B)^2, \quad (6)$$

where  $E_{A-A}$  and  $E_{B-B}$  are the homopolar bond energies and  $\chi_A$  and  $\chi_B$  are corresponding electronegativities. According to chemical bond approach [23], atoms combine more favorably with the atoms of different kind than with the same kind. Bonds are formed in order of decreasing bond energies thereby favoring chemical order. The base binary system contains Sb–Se and Se–Se bonds with energies 43.96 and 44 kcal mol<sup>-1</sup>, respectively [10]. On addition of Ge, additional Ge–Se bonds, having energy 49.92 kcal mol<sup>-1</sup>, start replacing Se–Se bonds resulting in an increase of cohesive energy,  $CE = \sum_i C_i E_i$ , where  $C_i$  is the distribution of chemical bonds and  $E_i$  is the energy associated with bonds. At  $x = 25$ , the system emerges as a 3D structure with maximum cohesive energy containing only Ge–Se and Sb–Se heteropolar bonds [10]. The increase in the cohesive energy enhances the bonding strength, therefore, increasing  $T_c$  and hence  $E_c$  up to  $x = 25$  [24]. The maximum value of  $E_c$  for  $\text{Sb}_{10}\text{Se}_{65}\text{Ge}_{25}$  indicates that atoms in its glassy state require more energy to jump to the crystalline phase. Therefore,  $\text{Sb}_{10}\text{Se}_{65}\text{Ge}_{25}$  is observed to be the most stable composition among investigated compositions. For  $x = 27$ , homopolar Ge–Ge bonds with energy 37.60 kcal mol<sup>-1</sup> are also formed leading to a decrease in the cohesive energy [10].

The decrease in cohesive energy of the system reduces  $T_c$  and hence,  $E_c$ . Therefore, the atoms require less energy to overcome the barrier, decreasing the stability.

The evaluated parameters suggest that the investigated glasses are thermally stable and offer a wide temperature range for various applications like in threshold switching [25, 26].

## Conclusions

Thermal studies have been carried out on  $\text{Sb}_{10}\text{Se}_{90-x}\text{Ge}_x$  ( $x = 0, 19, 21, 23, 25, 27$ ) under non-isothermal conditions using DTA. The three characteristic temperatures, glass transition ( $T_g$ ), crystallization ( $T_c$ ), and melting ( $T_m$ ) increase to maximum for  $x = 25$  and then decrease for  $x = 27$  at % Ge. This signifies an increase in the rigidity and resistance to devitrification of the glassy system. At  $x = 25$ ,  $T_c - T_g$  and activation energy of crystallization ( $E_c$ ) show maximum which indicates that this composition is thermally stable with a complete three dimensional network and is less prone to phase separation. These properties suggest that the composition with  $x = 25$  may be explored for threshold switching applications.

**Acknowledgments** The authors acknowledge Wadia Institute of Himalayan Geology, Dehradun for providing EDAX facility.

## References

1. Wakkad MM, Shokr EK, Abd El Ghani HA, Awad MA. Structural and kinetic evaluation of Sn-Sb-Se alloys. *J Phys D: Appl Phys.* 2007;40:7572–8.
2. Fritzsche H. Why are chalcogenide glasses the materials of choice for ovonic switching devices? *J Phys Chem Solids.* 2007;68:878–82.
3. Mott NF. *Electronic processes in non-crystalline materials.* London: Clarendon; 1979.
4. Zhimei S, Zhou J, Blomqvist A, Johansson B, Ahuja R. Fast crystallization of chalcogenide glass for rewritable memories. *Appl Phys Lett.* 2008;93:061913.
5. Chatterjee R, Asokan S, Titus SSK. Current controlled negative-resistance behavior and memory switching in bulk As–Se–Te glasses. *J Phys D: Appl Phys.* 1994;27:2624–7.
6. Kasap SO, Aiyah V, Yannacopoulos S. Thermal and mechanical properties of amorphous selenium films in the glass transformation region. *J Phys D Appl Phys.* 1989;23:553–61.
7. Sharma P, Sharma I, Katyal SC. Physical and optical properties of binary amorphous selenium-antimony thin films. *J Appl Phys.* 2009;105:053509.
8. Khushwaha N, Singh S, Shukla RK, Kumar A. Effect of Sb impurity on the photoelectrical properties of a-Se. *J Alloys Compd.* 2008;456:46–50.
9. Tonchev D, Kasap SO. Thermal properties of  $\text{Sb}_x\text{Se}_{90-x}$  glasses studied by modulated temperature differential scanning Calorimetry. *J Non-Cryst Solids.* 1999;248:28–36.
10. Sharda S, Sharma N, Sharma P, Sharma V. Physical analysis of structural transformation in Ge-incorporated a- $\text{Sb}_{10}\text{Se}_{90}$  system. *Defects and Diffusion Forum.* 2011;319–317:45–53.

11. Sharda S, Sharma N, Sharma P, Sharma V. Band gap and dispersive behavior of Ge alloyed *a-SbSe* thin films using single transmission spectrum. *Mater Chem Phys*. 2012;134:158–62.
12. Sharda S, Sharma N, Sharma P, Sharma V. Finger prints of chemical bonds in Sb–Se–Ge and Sb–Se–Ge–In glasses: a far-IR study. *J Non-Cryst Solids*. 2013;362:136–9.
13. Kumar R, Sharma P, Barman PB, Sharma V, Katyal SC, Rangra VS. Thermal stability and crystallization kinetics of SeTeSn alloys using differential scanning calorimetry. *J Therm Anal Calorim*. 2011;. doi:10.1007/s10973-011-2062-z.
14. Kaur G, Komatsu T, Thangaraj R. Crystallization kinetics of bulk amorphous Se–Te–Sn system. *J Mater Sci*. 2000;35:903–6.
15. Turnbull D. Under what conditions can a glass be formed? *Contemp Phys*. 1969;10:473–88.
16. Abd Elnaeim AM, Aly KA, Afify N, Abousehly AM. Glass transition and crystallization kinetics of  $\text{In}_x(\text{Se}_{0.75}\text{Te}_{0.25})_{100-x}$  chalcogenide glasses. *J Alloy Compd*. 2010;491:85–91.
17. Moynihan CT, Eastale AJ, Wilder J, Tucker J. Dependence of glass transition temperature on heating and cooling rate. *J Phys Chem*. 1974;78:2673–7.
18. Kissinger HE. Variation of peak temperature with heating rate in differential thermal analysis. *J Res Bur Stand*. 1956;57:217–21.
19. Al-Ghamdi AA, Alvi MA, Khan SA. Non-isothermal crystallization kinetic study on  $\text{Ga}_{15}\text{Se}_{85-x}\text{Ag}_x$  chalcogenide glasses by using differential scanning calorimetry. *J Alloy Compd*. 2011;509:2087–93.
20. Mahadevan S, Giridhar A, Singh AK. Calorimetric measurements on As–Sb–Se glasses. *J Non-Cryst Solids*. 1986;88:11–34.
21. Augis JA, Benett JE. Calculation of the Avrami parameters for heterogeneous solid state reactions using a modification of the Kissinger method. *J Therm Anal Calorim*. 1978;13:283–92.
22. Pauling L. The nature of chemical bond, Cornell University; New York: 1976.
23. Bicerano J, Ovshinsky SR. Chemical bond approach to glass structure. *J Non-Cryst Solids*. 1985;75:169–76.
24. Shaaban ER, Kansal I, Shapaan M, Ferreira JMF. Thermal stability and crystallization kinetics of ternary Se–Te–Sb semiconducting glassy alloys. *J Therm Anal Calorim*. 2009;98:347–54.
25. Kotkata MF, Mansour SA. Crystallization process analysis for  $\text{Se}_{0.95}\text{In}_{0.05}$  and  $\text{Se}_{0.90}\text{In}_{0.10}$  chalcogenide glasses using the contemporary isoconversional models. *J Therm Anal Calorim*. 2011;103:957–65.
26. Svoboda R, Malek J. Extended study of crystallization kinetics for Se-Te glasses. *J Therm Anal Calorim*. 2013;111:161–71.